

Generating 4-dimensional Wormholes with Yang-Mills Casimir Sources

A. C. L. Santos,^{1,*} R. V. Maluf,^{1,†} and C. R. Muniz^{2,‡}

¹*Universidade Federal do Ceará (UFC), Departamento de Física,
Campus do Pici, Fortaleza - CE, C.P. 6030, 60455-760 - Brazil.*

²*Universidade Estadual do Ceará (UECE),
Faculdade de Educação, Ciências e Letras de Iguatu,
Av. Dário Rabelo s/n, Iguatu-CE, 63.500-000 - Brazil.*

(Dated: August 29, 2024)

Abstract

This work presents a new static and spherically symmetric traversable wormhole solution in General Relativity, which is supported by the quantum vacuum fluctuations associated with the Casimir effect of the Yang-Mills field confined between perfect chromometallic mirrors in $(3 + 1)$ dimensions, recently fitted using first-principle numerical simulations. Initially, we employ a perturbative approach for $x = mr \ll 1$, where m represents the Casimir mass and r is the radial coordinate. This approach has proven to be a reasonable approximation when compared with the exact case in this regime. To find well-behaved redshift functions, we impose constraints on the free parameters. As expected, this solution recovers the electromagnetic-like Casimir solution for $m = 0$. Analyzing the traversability conditions, we graphically find that all are satisfied for $0 \leq m \leq 0.17$. On the other hand, all the energy conditions are violated, as usual in this context due to the quantum origin of the source. Stability from Tolman-Oppenheimer-Volkov (TOV) equation is guaranteed for all r and from the speed of sound for $0.16 \leq m \leq 0.18$. Therefore, for $0.16 \leq m \leq 0.17$, we will have a stable solution that satisfies all traversability conditions.

Keywords: General Relativity. Yang-Mills Field. Casimir Effect. Wormholes.

*Electronic address: alanasantos@fisica.ufc.br

†Electronic address: r.v.maluf@fisica.ufc.br

‡Electronic address: celio.muniz@uece.br

I. INTRODUCTION

Some inconsistencies within the framework of General Relativity have demanded severe efforts from physicists. Singularities and the incompatibility with observations in the cosmological scenario, among others, have guided different proposals: adding new invariants or fields, exploring alternative geometries and quantization (a great compilation can be found in [1]). However, faced with these problems, we inquire: Are we adequately comprehending and describing the vacuum structure? What effects could arise when we include experimentally confirmed quantum vacuum effects?

One of the most established effects is called the Casimir effect and is associated with quantum vacuum fluctuations when we impose boundary conditions [2]. Over the years, studies have emerged to investigate the effect of curved spaces on Casimir energy density [3–6]. On the other hand, following Garattini’s work, this energy density and the associated pressure was incorporated as source in Einstein’s equations, resulting in the formation of wormholes for the Casimir effect of the electromagnetic field in $(3 + 1)$ [7], $(2 + 1)$ [8] and D dimensions [9]. Also with the Casimir effect of the Yang-Mills field in $(2 + 1)$ dimensions [10] and extensions of General Relativity [11–17].

Wormholes are hypothetical structures that would connect two distinct regions of space-time. However, unlike Black Holes, which already have observational confirmation and well-established sources provided by stellar evolution [18, 19], wormholes suffer from a series of questions, including a natural formation process. In 1988, Morris and Thorne conducted a detailed study of the characteristics this hypothetical structure would need to possess in order to be traversable [20]. They concluded that it would require negative energy density - exotic matter - which at the time increased the skepticism related to this solution. Interestingly, one of the characteristics of the Casimir energy density is that for certain configurations, it can assume negative values. This is why it has been proposed as a potential source for this solution.

In this sense, based on the previously mentioned results, this work aims to restate the possibility of a wormhole formation with a new source given by the Casimir energy density and the corresponding pressure of the Yang-Mills field in $(3 + 1)$ dimensions. This quantity was recently obtained through first-principles numerical simulations in Lattice QCD, where it was identified that the Casimir interaction between perfect chromometallic mirrors reveals

the presence of a new gluonic state with a mass of $m = 0.49(5)$ GeV [21]. On the other hand, due to the numerical difficulties in treating the solution exactly and taking into account that this effect occurs at microscopic distances for small masses, on considering a gravitational scenario we will make a perturbative approach for $x = mr \ll 1$, and to eliminate the singularities that arise at the throat - common in this context - we will impose a constraint on the free parameters.

Our paper is organized as follows: In section II, considering a perturbative approach, we find the shape and redshift functions, analyzing how the Casimir mass influences the wormhole characteristics. In section III, to identify the physical consistency of this solution, we investigated the traversability conditions, energy conditions, stability from the speed of sound, and TOV equation. Finally, in section IV we outline our conclusions.

II. WORMHOLE SOLUTION

Since we are going to consider General Relativity, we begin by defining the well-known Einstein-Hilbert action in $(3 + 1)$ dimensions

$$S = \frac{1}{16\pi} \int d^4x \sqrt{-g} (R + \mathcal{L}_m), \quad (1)$$

where g stands for the determinant of the metric $g_{\mu\nu}$, R is the Ricci scalar and \mathcal{L}_m is the Lagrangian density of matter. Varying (1) concerning the metric, we obtain the equations of motion

$$R^\mu_\nu - \frac{1}{2} g^\mu_\nu R = \kappa T^\mu_\nu, \quad (2)$$

with $\kappa = 8\pi$, where $G = \hbar = c = 1$. Assuming that the Casimir energy density and pressures effectively act as a fluid with density $\rho(r)$, radial pressure $p_r(r)$, and tangential pressure $p_t(r)$, we will consider:

$$T^\mu_\nu = \text{diag} (-\rho(r), p_r(r), p_t(r), p_t(r)). \quad (3)$$

Let us assume a spherically symmetric and static ansatz for the spacetime metric with the line element given by

$$ds^2 = -e^{2\Phi(r)} dt^2 + \frac{1}{1 - \frac{b(r)}{r}} dr^2 + r^2 d\theta^2 + r^2 \sin^2 \theta d\phi^2, \quad (4)$$

which represents a $(3 + 1)$ -dimensional Morris-Thorne wormhole [20], where the redshift function $\Phi(r)$ and the shape function $b(r)$ are arbitrary functions of the polar coordinate $r \in [r_0, +\infty)$. Thus, the coordinate r must be decreased from infinity to a minimum value r_0 , the radius of the throat. Replacing the ansatz to the metric (4) and the energy-momentum tensor (3) in the Einstein field equations (2), we find

$$\frac{b'(r)}{r^2} = \kappa\rho(r), \quad (5)$$

$$\kappa p_r(r) = -\frac{b(r)}{r^3} + \frac{2\Phi'(r)}{r} - \frac{2b(r)\Phi'(r)}{r^2}, \quad (6)$$

$$\left(1 - \frac{b(r)}{r}\right) \left(\Phi''(r) + \Phi'^2(r) + \frac{\Phi'(r)}{r}\right) - \frac{b'(r)r - b(r)}{2r^2} \left(\Phi'(r) + \frac{1}{r}\right) = \kappa p_t(r). \quad (7)$$

The prime ($'$) stands for the total derivative concerning the radial coordinate r . On the other hand, the covariant energy-momentum conservation law leads to

$$p_r'(r) = \frac{-2p_r(r) + 2p_t(r) - r(p_r(r) + \rho(r))\Phi'(r)}{r}. \quad (8)$$

We will consider as a source the Casimir energy in non-Abelian gauge theory described as the Casimir energy of a massive scalar particle with certain mass m which was recently fitted using first-principles numerical simulations [21]

$$\frac{\mathcal{E}_{Cas}}{S} = \sum_{n=1}^{\infty} -\frac{2C_0 m^2}{\pi^2 r} \frac{K_2(2nmr)}{n^2}, \quad (9)$$

where S is the surface of the plates, C_0 is a phenomenological parameter, r is the distance between the plates and $K_2(z)$ gives the modified Bessel function of the second kind. The analysis provides the following best-fit parameters: $C_0 = 5.60(7)$ and $m = 0.49(5)$ GeV. Due to the numerical difficulties encountered when dealing with this expression exactly, we will use the perturbative approach considering $x = mr$, for $x \ll 1$ [22]. In this limit, the asymptotic behavior of the modified Bessel function for a fixed value of n can be described by [23]:

$$K_2(2nmr) = \frac{2}{(nmr)^2} - \frac{1}{2} + O(m^2). \quad (10)$$

Substituting into the summation over n , we obtain the following Casimir energy [24]:

$$\frac{\mathcal{E}_{Cas}(m \ll r^{-1})}{S} = -\frac{\pi^4 \lambda}{180r^3} + \frac{15\pi^2 \lambda x^2}{180r^3} + O(x^4), \quad (11)$$

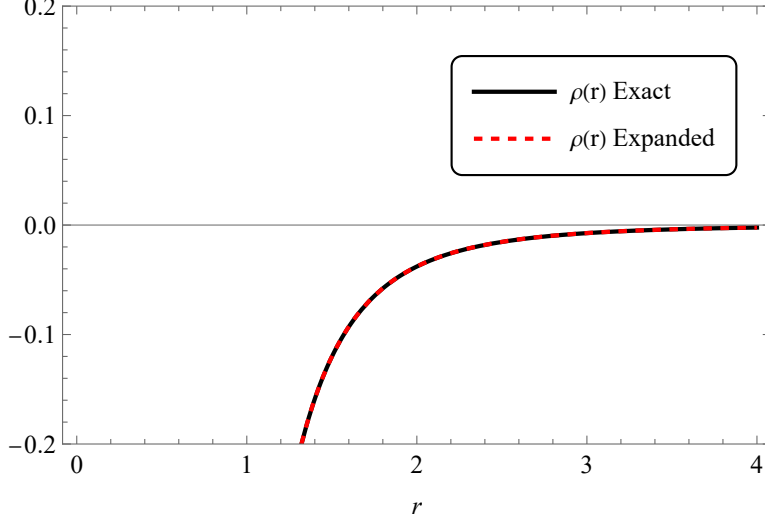


Figure 1: The graphical representation of the radial dependence for $\rho(r)$ exact and expanded, with $n = 1, \dots, 100$, $C_0 = 5.6$ and $m = 5 \times 10^{-2}$.

where,

$$\lambda = \frac{2C_0}{\pi^2}. \quad (12)$$

In which the first term is associated with the Casimir energy of a massless scalar field. Finally we can obtain the Casimir energy density

$$\rho(m \ll r^{-1}) = \frac{\mathcal{E}_{Cas}(m \ll r^{-1})}{Sr} = -\frac{\pi^2 \lambda (\pi^2 - 15m^2 r^2)}{180r^4}. \quad (13)$$

To confirm the accuracy of this density as an approximation of the exact function within this regime, we generated a comparative graph depicted in Figure 1. This graph juxtaposes the exact densities with those expanded using the best fit parameters C_0 and $m = 5 \times 10^{-2}$ [21]. Through this comparison, we can confidently assert its validity as a reliable approximation.

From (5) and (13) we obtain the shape function

$$b(m \ll r^{-1}) = \frac{\pi^2 \kappa \lambda (r - r_0) (15r_0 m^2 r - \pi^2)}{180r_0 r} + r_0. \quad (14)$$

The constant of integration was fixed such that the throat condition $b(r_0) = r_0$ is satisfied. When $m \rightarrow 0$, we recover the profile of the wormhole solution sustained by the Casimir effect of the electromagnetic field, as expected [7]. Besides this, we observe that in the limit $r \rightarrow \infty$ the expression

$$\frac{b(r)}{r} \approx \frac{\pi^2 \kappa \lambda m^2}{12}, \quad (15)$$

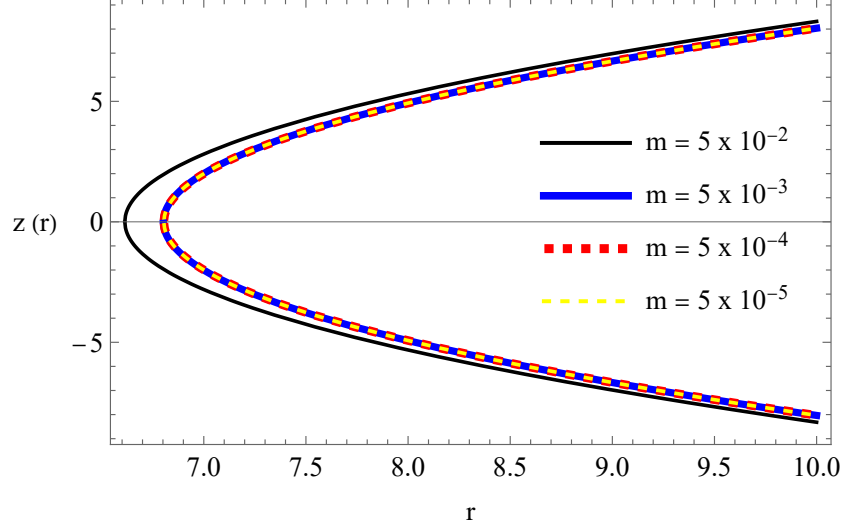


Figure 2: Representation of the embedding diagram with different values of m , with $C_0 = 5.6$ and r_0 given by (20), in natural units where $G = \hbar = c = 1$.

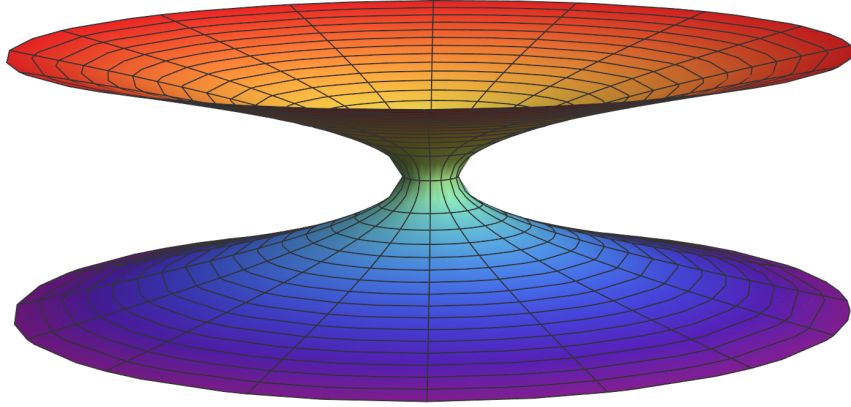


Figure 3: Embedded shape of the (3+1) Casimir-Yang-Mills wormhole with $m = 5 \times 10^{-2}$, $C_0 = 5.6$ and r_0 given by (20), in natural units where $G = \hbar = c = 1$.

indicates that the spacetime exhibits a defect in the solid angle, similar to the behavior of a global monopole, for sufficiently large distances from the throat. This characteristic arises due to the non-trivial topology introduced by the quantum fluctuations of the Yang-Mills field, which modifies the angular structure of the spacetime and leads to a deficit angle. Note that this feature does not occur when $m \rightarrow 0$, corresponding to the usual electromagnetic limit.

Analyzing Figure 2, which depicts embedding diagrams for different values of m , we identified that the larger the Casimir mass, the smaller the throat radius, which aligns with the constraint given by the equation (20) and can be interpreted as an increase in m leading to more intense quantum effects, causing pronounced distortions in the geometry of the wormhole. However, very tiny masses have a throat radius that is very close due to the dependence of r_0 with the inverse of m^2 . Figure 3 represents this three-dimensional embedding, highlighting its asymptotic flatness.

Let us turn our attention to the redshift function associated with the Casimir-Yang Mills wormhole. The radial pressure is given by

$$p_r(m \ll r^{-1}) = -\frac{1}{S} \frac{d\mathcal{E}_{Cas}}{dr} = -\frac{\pi^2 \lambda (\pi^2 - 5m^2 r^2)}{60r^4}. \quad (16)$$

This allows us to conclude the following equation of state:

$$p_r(m \ll r^{-1}) = \omega(m \ll r^{-1})\rho(m \ll r^{-1}); \quad \omega(m \ll r^{-1}) = \frac{2\pi^2}{\pi^2 - 15m^2 r^2} + 1, \quad (17)$$

which recovers the ω of the electromagnetic case for $m = 0$, as expected. From (6), (14) and (16) we obtain

$$\begin{aligned} \Phi(m \ll r^{-1}) &= \frac{1}{2(\pi^2 \kappa \lambda m^2 - 12)(\pi^4 \kappa \lambda - 15r_0^2(\pi^2 \kappa \lambda m^2 - 12))} \\ &\times \left(3 \ln(r - r_0) (\pi^2 \kappa \lambda m^2 - 12) (5r_0^2 (\pi^2 \kappa \lambda m^2 + 12) - \pi^4 \kappa \lambda) \right. \\ &+ \left(45r_0^2 (\pi^2 \kappa \lambda m^2 - 12)^2 - \pi^4 \kappa \lambda (\pi^2 \kappa \lambda m^2 + 12) \right) \ln(15r_0 r (\pi^2 \kappa \lambda m^2 - 12) - \pi^4 \kappa \lambda) \\ &\left. + \ln(r) + c_1, \right. \end{aligned} \quad (18)$$

where c_1 is a constant. In order to have a traversable wormhole we need to eliminate the divergence in the logarithmic term at $r \rightarrow r_0$, which implies the constraint

$$5r_0^2 (\pi^2 \kappa \lambda m^2 + 12) - \pi^4 \kappa \lambda = 0, \quad (19)$$

which leads

$$r_0 = \pi^2 \sqrt{\frac{\kappa \lambda}{5\pi^2 \kappa \lambda m^2 + 60}}. \quad (20)$$

Considering (19), the redshift function becomes:

$$\begin{aligned} \Phi(m \ll r^{-1}) &= \frac{2(\pi^2 \kappa \lambda m^2 - 6) \ln(10r_0^2 (\pi^2 \kappa \lambda m^2 - 24))}{\pi^2 \kappa \lambda m^2 - 12} + \ln\left(\frac{r}{r_0}\right) + 1 \\ &- \frac{2(\pi^2 \kappa \lambda m^2 - 6) \ln(-5\pi^2 r_0 \kappa \lambda m^2 (r_0 - 3r) - 60r_0(r_0 + 3r))}{\pi^2 \kappa \lambda m^2 - 12}, \end{aligned} \quad (21)$$

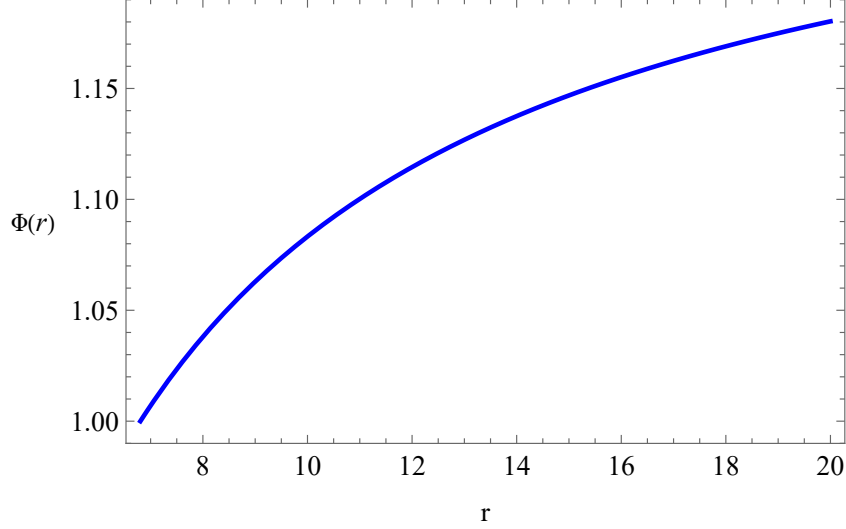


Figure 4: Redshift function from equation (21) with $m = 5 \times 10^{-4}$, $C_0 = 5.6$ and r_0 given by (20), in natural units where $G = \hbar = c = 1$.

which is a finite quantity when $r \rightarrow r_0$. The constant of integration c_1 was fixed such that $\Phi(r_0) = 1$ is satisfied. This behavior is illustrated in Figure 4. Note that for the argument of the first logarithm we have the condition $\pi^2 \kappa \lambda m^2 \neq 24$ and for the second logarithm to be null, we need

$$5\pi^2 r_0 \kappa \lambda m^2 (3r - r_0) - 60r_0(r_0 + 3r) = 0, \quad (22)$$

which implies,

$$r = r_0 \left(\frac{8}{\pi^2 \kappa \lambda m^2 - 12} + \frac{1}{3} \right) < r_0. \quad (23)$$

It is valid to mention that for $m \rightarrow 0$, we recover the solution profile sustained by the electromagnetic Casimir source [7]. Certainly, the redshift function will diverge as $r \rightarrow \infty$ due to the presence of the second logarithmic term. However, in this limit, the approximation $x = mr \ll 1$ is no longer valid. Therefore, we cannot use (13) to describe the Casimir energy density and, consequently, (21) as a solution to the redshift function. Since the Kretschmann scalar is an involved expression, to ensure the absence of singularities in this spacetime for this regime we plotted Figure 5.

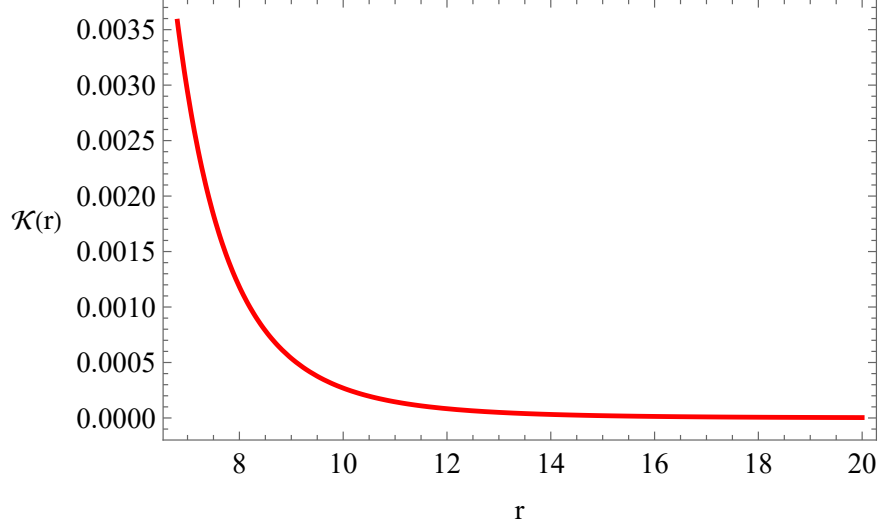


Figure 5: Kretschmann scalar with $m = 5 \times 10^{-4}$, $C_0 = 5.6$ and r_0 given by (20), in natural units where $G = \hbar = c = 1$.

III. SOURCE PROPERTIES

A. Traversability Conditions

Let's investigate whether the conditions established for traversability [20] are satisfied by the redshift and shape functions found.

(i) A flaring-out condition, associated with the minimality of the wormhole throat, implies that

$$\frac{b(r) - rb'(r)}{b(r)^2} = -\frac{180r_0r(-15r_0^2r(12 - \pi^2\kappa\lambda m^2) - 2\pi^4r_0\kappa\lambda + \pi^4\kappa\lambda r)}{(180r_0^2r + \pi^2\kappa\lambda(r_0 - r)(\pi^2 - 15r_0m^2r))^2} > 0. \quad (24)$$

And on the throat

$$b'(r_0) = \frac{1}{180}\pi^2\kappa\lambda \left(15m^2 - \frac{\pi^2}{r_0^2} \right) < 1. \quad (25)$$

(ii) Another condition is given by

$$1 - \frac{b(r)}{r} = \frac{(r - r_0)(15r_0r(12 - \pi^2\kappa\lambda m^2) + \pi^4\kappa\lambda)}{180r_0r^2} \geq 0. \quad (26)$$

We plotted a graph in Figure 6 to analyze which values of m allow the conditions (24), (25), and (26) to be satisfied within the approach. Thus, we can conclude that for $0 \leq m \leq 0.17$, all traversability conditions will be satisfied, which is consistent with the approximation we are employing. On the other hand, the shape function is asymptotically flat-like, since

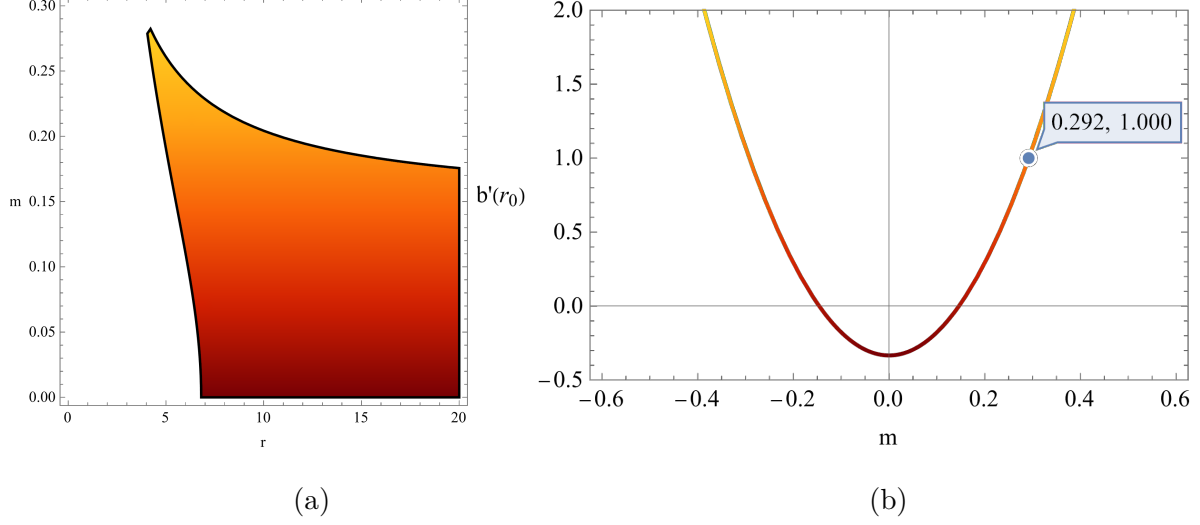


Figure 6: Region where the traversability conditions given by (24), (26) (a) and (25) (b) are satisfied with $C_0 = 5.6$ and r_0 given by (20), in natural units where $G = \hbar = c = 1$.

$$\lim_{r \rightarrow \infty} \left(1 - \frac{b(r)}{r} \right) = 1 - \frac{\pi^2 \kappa \lambda m^2}{12}. \quad (27)$$

Despite exhibiting the desired behavior, as mentioned earlier, the asymptotic limit $r \rightarrow \infty$ does not fit within the approximation we are using. Finally, from (7), (14) and (18) and imposing the constraint (20), we can obtain the tangential pressure:

$$p_t(m \ll r^{-1}) = -\frac{\pi^2 \lambda (3\pi^2 r (5\kappa \lambda m^2 (\pi^2 - 3m^2 r^2) - 36) - \alpha (15m^2 r^2 + \pi^2))}{180r^4 (\alpha + r (36 - 3\pi^2 \kappa \lambda m^2))}, \quad (28)$$

where,

$$\alpha = \pi^2 \sqrt{\frac{\kappa \lambda (\pi^2 \kappa \lambda m^2 + 12)}{5}}. \quad (29)$$

It is worth mentioning that the same result is found using the equation (8), as expected. Therefore, the Casimir source that generates a wormhole effectively acts as an anisotropic fluid, since the radial and tangential pressures are distinct as evidenced by the the equations (16) and (28). This is in agreement with analysis in more general contexts [25].

B. Energy Conditions

The energy conditions state that for a given fluid with density $\rho(r)$, radial pressure $p_r(r)$, and lateral pressures $p_t(r)$, the following relationships must be satisfied: $\rho(r) \geq 0$

and $\rho(r) + p_i(r) \geq 0$ (Weak Energy Condition), $\rho(r) + p_i(r) \geq 0$ (Null Energy Condition), $\rho(r) + \sum_i p_i(r) \geq 0$ and $\rho(r) + p_i(r) \geq 0$ (Strong Energy Condition) and $\rho(r) - |p_i(r)| \geq 0$ (Dominant Energy Condition).

As we can see in Figure 7, all the energy conditions will be violated. This fact is common in other contexts of wormholes sustained by the Casimir source and is reasonable since these conditions have a classical nature, whereas the analyzed source has a quantum origin.

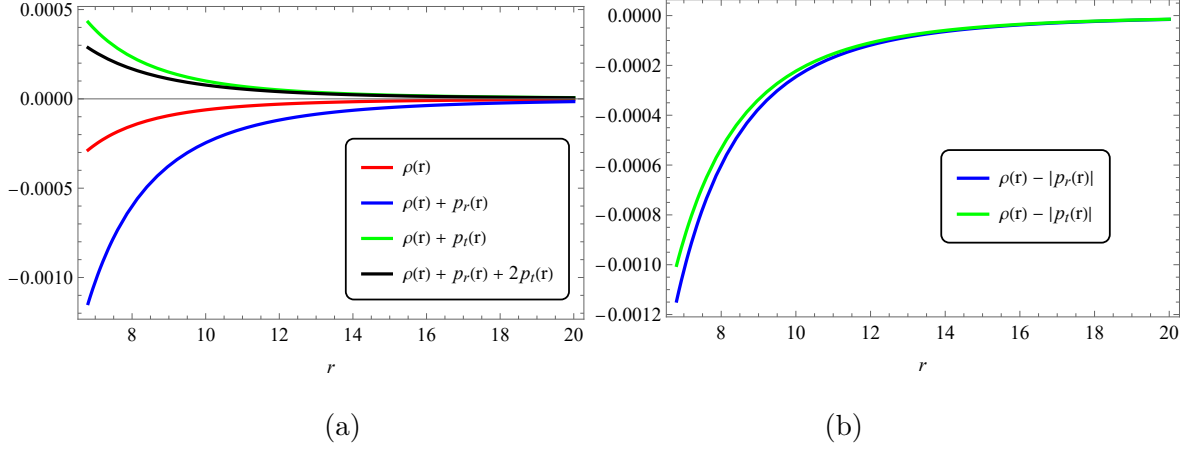


Figure 7: The graphical representation of the radial dependence for a combination of density and pressures (a) and (b) with r_0 given by (20), $m = 5 \times 10^{-4}$ and $C_0 = 5.6$, in natural units where $G = \hbar = c = 1$.

C. Stability from sound velocity

In order to evaluate the stability of the Casimir wormhole, we must first analyze the condition described by the expression [26, 27]:

$$v_s^2(r) = \frac{1}{3} \left[\frac{d(p_r + 2p_t)}{d\rho} \right] = \frac{1}{3} \left[\frac{p'_r(r) + 2p'_t(r)}{\rho'(r)} \right] \geq 0, \quad (30)$$

with v_s representing the sound velocity in the medium. Considering (13), (16) and (28) we obtain

$$v_s^2(r) = \frac{-15m^2r^2 + \gamma(r)}{3(2\pi^2 - 15m^2r^2)} \geq 0, \quad (31)$$

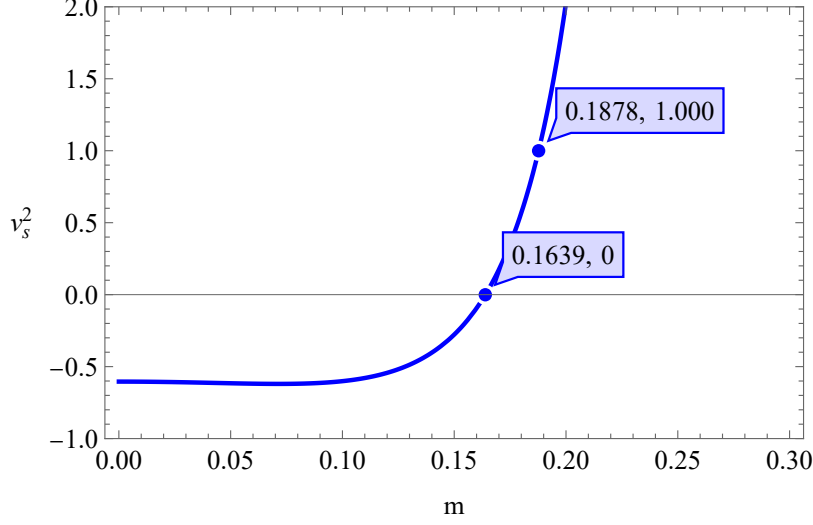


Figure 8: Graphical representation of v_s^2 with $r \approx r_0$ given by (20) and $C_0 = 5.6$, in natural units where $G = \hbar = c = 1$.

where,

$$\begin{aligned} \gamma(r) = & \frac{1}{\left(\pi^2 \sqrt{5(\kappa \lambda \pi^2 \kappa \lambda m^2 + 12)} - 15r (\pi^2 \kappa \lambda m^2 - 12)\right)^2} \\ & \times \left(10\pi^2 \left(45\sqrt{5\kappa \lambda} m^2 r^3 (\pi^2 \kappa \lambda m^2 - 18) \sqrt{\pi^2 \kappa \lambda m^2 + 12} + 675\kappa \lambda m^4 r^4 (\pi^2 \kappa \lambda m^2 - 12)\right.\right. \\ & + \pi^4 \kappa \lambda (\pi^2 \kappa \lambda m^2 + 12) + 12\pi^2 \sqrt{5\kappa \lambda} r (\pi^2 \kappa \lambda m^2 - 3) \sqrt{\pi^2 \kappa \lambda m^2 + 12} \\ & \left.\left. - 30r^2 (\pi^2 \kappa \lambda m^2 - 6) (11\pi^2 \kappa \lambda m^2 - 108)\right)\right). \end{aligned} \quad (32)$$

Since stability must be analyzed in the throat, let's consider $r \approx r_0$, where r_0 is given by (20), and examine in the Figure 8 which values of m allow for a stable solution. As we can identify, to satisfy the condition given by (30) and avoid superluminal velocities, we need $0.16 \leq m \leq 0.18$. Therefore, for $0.16 \leq m \leq 0.17$ we have a stable solution with the traversability conditions satisfied.

D. Stability from TOV equation

From (8), we can identify:

$$\mathcal{F}_g + \mathcal{F}_h + \mathcal{F}_a = 0, \quad (33)$$

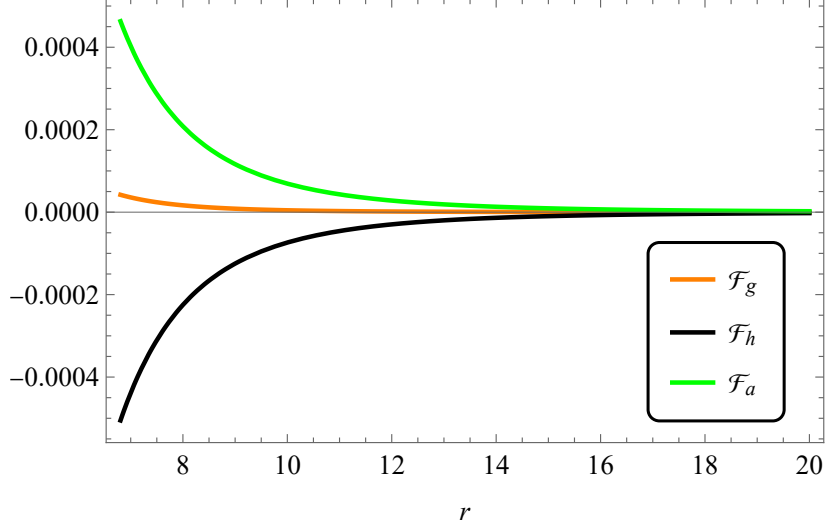


Figure 9: The graphical representation of \mathcal{F}_g , \mathcal{F}_h and \mathcal{F}_a as functions of the radial coordinate r , with r_0 given by (20), $m = 5 \times 10^{-4}$ and $C_0 = 5.6$, in natural units where $G = \hbar = c = 1$.

where,

$$\mathcal{F}_g = -\Phi'(r)(\rho(r) + p_r(r)); \mathcal{F}_h = -\frac{dp_r(r)}{dr}; \mathcal{F}_a = \frac{-2(p_r(r) - p_t(r))}{r}, \quad (34)$$

with \mathcal{F}_h the hydrostatic force, \mathcal{F}_g the gravitational force and \mathcal{F}_a the anisotropic force. It is straightforward to verify that our traversable wormhole solution satisfies the TOV equation with r_0 given by (20). The profiles of \mathcal{F}_g , \mathcal{F}_h and \mathcal{F}_a are depicted in Figure 9. \mathcal{F}_a and \mathcal{F}_g take positive values near the throat, while \mathcal{F}_h is negative, clearly indicating that to maintain the system in an equilibrium state, the hydrostatic force is balanced by the combined effect of gravitational and the anisotropic forces, in a similar behavior of $(2 + 1)$ dimensions [10].

IV. CONCLUSION

In summary, we have found a wormhole solution supported by the energy density and Casimir pressures associated with the Yang-Mills field, which has recently been simulated using first-principles numerical simulations in $(3 + 1)$ dimensions. We considered a perturbative approach for $x = mr \ll 1$, where m is the Casimir mass and r is the radial coordinate. To eliminate the divergence of the redshift function at the throat, we imposed a constraint on its radius, r_0 . We identified in the shape function that a larger Casimir mass implies a smaller wormhole throat. This function also demonstrates that asymptotically,

the Yang-Mills Casimir wormhole exhibits a defect in the solid angle, similar to a global monopole.

In order to the traversability conditions to be satisfied, it is necessary $0 \leq m \leq 0.17$, which is consistent with the approximation considered. In turn, the solution is stable for all r from the point of view of TOV equation, as well as of the speed sound for $0.16 \leq m \leq 0.18$. Thus, considering $0.16 \leq m \leq 0.17$ for the Casimir mass implies that we will have a stable solution that satisfies all traversability conditions. We have also shown that all the energy conditions are violated, which is typical in this context due to the quantum nature of the source. For $m = 0$, we recover the expected Casimir electromagnetic solution.

To conclude, quantum vacuum fluctuations and non-linearities associated with the Yang-Mills field within hadrons could enable and stabilize submicroscopic wormholes by providing the appropriate negative energy. Although their detection remains challenging, indirect methods may uncover their presence through tiny deviations in high-energy particle collisions. Our research will seek using quasinormal modes (QNMs) to investigate the wormhole responses to perturbations, which would help guide experimental design and refine detection techniques.

Acknowledgments

The authors thank the Fundação Cearense de Apoio ao Desenvolvimento Científico e Tecnológico (FUNCAP), the Coordenação de Aperfeiçoamento de Pessoal de Nível Superior (CAPES), and the Conselho Nacional de Desenvolvimento Científico e Tecnológico (CNPq), Grants no. 88887.822058/2023-00 (ACLS), no. 308268/2021-6 (CRM), and no. 200879/2022-7 (RVM) for financial support.

-
- [1] E. N. Saridakis *et al.* [CANTATA], Springer, 2021, ISBN 978-3-030-83714-3, 978-3-030-83717-4, 978-3-030-83715-0 doi:10.1007/978-3-030-83715-0 [[arXiv:2105.12582](#) [gr-qc]].
 - [2] H. B. G. Casimir, *Indag. Math.* **10** (1948) no.4, 261-263
 - [3] F. Sorge, *Int. J. Mod. Phys. D* **29** (2019) no.01, 2050002 doi:10.1142/S0218271820500029
 - [4] A. C. L. Santos, C. R. Muniz and L. T. Oliveira, *Int. J. Mod. Phys. D* **30** (2021) no.05, 2150032 doi:10.1142/S0218271821500322 [[arXiv:2007.00227](#) [gr-qc]].

- [5] A. C. L. Santos, C. R. Muniz and L. T. Oliveira, EPL **135** (2021) no.1, 19002 doi:10.1209/0295-5075/135/19002 [[arXiv:2103.03368](#) [gr-qc]].
- [6] H. F. S. Mota, C. R. Muniz, and V. B. Bezerra, Universe **8**, 11, 597 (2022), doi:10.3390/universe8110597, [arXiv: 2210.06128 [hep-th]].
- [7] R. Garattini, Eur. Phys. J. C **79** (2019) no.11, 951 doi:10.1140/epjc/s10052-019-7468-y [[arXiv:1907.03623](#) [gr-qc]].
- [8] G. Alencar, V. B. Bezerra and C. R. Muniz, Eur. Phys. J. C **81** (2021) no.10, 924 doi:10.1140/epjc/s10052-021-09734-0 [[arXiv:2104.13952](#) [gr-qc]].
- [9] P. H. F. Oliveira, G. Alencar, I. C. Jardim and R. R. Landim, Mod. Phys. Lett. A **37** (2022) no.15, 2250090 doi:10.1142/S0217732322500900 [[arXiv:2107.00605](#) [hep-th]].
- [10] A. C. L. Santos, C. R. Muniz and R. V. Maluf, JCAP **09** (2023), 022 doi:10.1088/1475-7516/2023/09/022 [[arXiv:2304.11131](#) [gr-qc]].
- [11] M. B. Cruz, R. M. P. Neves and C. R. Muniz, JCAP **05** (2024), 016 doi:10.1088/1475-7516/2024/05/016 [[arXiv:2401.08885](#) [gr-qc]].
- [12] Z. Hassan, S. Ghosh, P. K. Sahoo and V. S. H. Rao, Gen. Rel. Grav. **55** (2023) no.8, 90 doi:10.1007/s10714-023-03139-y [[arXiv:2209.02704](#) [gr-qc]].
- [13] M. Zubair, S. Waheed, M. Farooq, A. H. Alkhaldi and A. Ali, Eur. Phys. J. Plus **138** (2023) no.10, 902 doi:10.1140/epjp/s13360-023-04539-4
- [14] Z. Hassan, S. Ghosh, P. K. Sahoo and K. Bamba, Eur. Phys. J. C **82** (2022) no.12, 1116 doi:10.1140/epjc/s10052-022-11107-0 [[arXiv:2207.09945](#) [gr-qc]].
- [15] S. K. Tripathy, Phys. Dark Univ. **31** (2021), 100757 doi:10.1016/j.dark.2020.100757 [[arXiv:2004.14801](#) [gr-qc]].
- [16] H. Azmat, Q. Muneer, M. Zubair, E. Gudekli, I. Ahmad and S. Waheed, Nucl. Phys. B **998** (2024), 116396 doi:10.1016/j.nuclphysb.2023.116396
- [17] A. K. Mishra, Shweta and U. K. Sharma, Universe **9** (2023) no.4, 161 doi:10.3390/universe9040161 [[arXiv:2303.04641](#) [physics.gen-ph]].
- [18] K. Akiyama *et al.* [Event Horizon Telescope], Astrophys. J. Lett. **875** (2019) no.1, L4 doi:10.3847/2041-8213/ab0e85 [[arXiv:1906.11241](#) [astro-ph.GA]].
- [19] K. Akiyama *et al.* [Event Horizon Telescope], Astrophys. J. Lett. **930** (2022) no.2, L12 doi:10.3847/2041-8213/ac6674 [[arXiv:2311.08680](#) [astro-ph.HE]].
- [20] M. S. Morris and K. S. Thorne, Am. J. Phys. **56** (1988), 395-412 doi:10.1119/1.15620

- [21] M. N. Chernodub, V. A. Goy, A. V. Molochkov and A. S. Tanashkin, Phys. Rev. D **108** (2023) no.1, 014515 doi:10.1103/PhysRevD.108.014515 [[arXiv:2302.00376](#) [hep-lat]].
- [22] R. V. Maluf, D. M. Dantas and C. A. S. Almeida, Eur. Phys. J. C **80** (2020) no.5, 442 doi:10.1140/epjc/s10052-020-8020-9 [[arXiv:1905.04824](#) [hep-th]].
- [23] M. Abramowitz and I. A. Stegun. Dover, New York, 1972.
- [24] G. Plunien, B. Muller and W. Greiner, Phys. Rept. **134** (1986), 87-193 doi:10.1016/0370-1573(86)90020-7
- [25] H. C. Kim and Y. Lee, JCAP **09** (2019), 001 doi:10.1088/1475-7516/2019/09/001 [[arXiv:1905.10050](#) [gr-qc]].
- [26] S. Capozziello, O. Luongo and L. Mauro, Eur. Phys. J. Plus **136** (2021) no.2, 167 doi:10.1140/epjp/s13360-021-01104-9 [[arXiv:2012.13908](#) [gr-qc]].
- [27] S. Capozziello, and N. Godani, Phys. Lett. **B835**, 137572 (2022), doi:10.1016/j.physletb.2022.137572, [[arXiv:2211.06481](#) [gr-qc]].